

KINGFISH  
Key Insights on Nearby Galaxies: a Far Infrared Survey with  
Herschel  
Data Products Delivery DR3  
Users Guide

October 21, 2013

## 1 Introduction

This document includes descriptions of both the second delivery (DR2) and the third delivery (DR3) of the high level data products of the Herschel Open Time Key Project KINGFISH (Key Insights on Nearby Galaxies: a Far Infrared Survey with Herschel; P.I.: R.C. Kennicutt; Deputy-P.I.: D. Calzetti) to the Herschel Science Center. The second delivery contained all imaging (PACS and SPIRE) products, while the third delivery, which is the subject of most updates to this document, contains PACS spectroscopy data products. A small calibration update is also reported for the SPIRE imaging products.

KINGFISH consists of a sample of 61 galaxies (the SPIRE maps for 6 of which, NGC4254, NGC4321, NGC4536, NGC4569, NGC4579, and NGC4725, were obtained as part of the Eales et al. Herschel Reference Survey and re-reduced by us), which have been mapped with both PACS (3 bands) and SPIRE (3 bands) and measured spectroscopically with PACS. DR2 included the PACS and SPIRE imaging of the 61 galaxies in KINGFISH, except for the PACS maps of NGC584, whose original observations failed and has been re-observed. DR3 includes the PACS Spectral data of the 54 galaxies for which spectral PACS spectral mapping was performed.

More details can be found in the paper by Kennicutt et al. (2011, PASP, 123, 1347).

## 2 Content of the PACS SPEC Data Delivery

### 2.1 Sample and Summary of Data Products

The galaxies in the KINGFISH sample are listed in Table 1. The galaxies for which spectra were obtained as part of the KINGFISH sample are listed in Table 2.

DR2 contains both PACS and SPIRE images in 3 bands each (70, 100, and 160  $\mu\text{m}$  for PACS, and 250, 350, and 500  $\mu\text{m}$  for SPIRE) for the galaxies in the sample. For galaxies in the spectral sample, DR3 contains cubes and maps of 4 spectral lines ([O I] 63 $\mu\text{m}$ , [O III] 88 $\mu\text{m}$ , [N II] 121 $\mu\text{m}$ , [C II] 158 $\mu\text{m}$ ). Spectral maps were centered on the nuclei of galaxies. In some galaxies these nuclear maps were extended in radial strips. Additional extra-nuclear regions were also targeted in select galaxies. The brightest targets also feature a 5<sup>th</sup> spectral line ([N II] 205 $\mu\text{m}$ ) which was observed in regions with the highest surface brightness. Summaries of the data products are given below, and details on the data processing are provided in sections 3, 4, and 5.

Table 1: Galaxies in the KINGFISH sample (listed in order of increasing RA)

Name	Name	Name	Name	Name	Name
NGC0337	IC0342	NGC3049	NGC3627	NGC4625	NGC5474
NGC0584	NGC1482	NGC3077	NGC3773	NGC4631	NGC5713
NGC0628	NGC1512	M81DwB	NGC3938	NGC4725	NGC5866
NGC0855	NGC2146	NGC3190	NGC4236	NGC4736	NGC6946
NGC0925	HolmbergII	NGC3184	NGC4254	DDO154	NGC7331
NGC1097	DDO053	NGC3198	NGC4321	NGC4826	NGC7793
NGC1266	NGC2798	IC2574	NGC4536	DDO165	
NGC1291	NGC2841	NGC3265	NGC4559	NGC5055	
NGC1316	NGC2915	NGC3351	NGC4569	NGC5398	
NGC1377	HolmbergI	NGC3521	NGC4579	NGC5408	
NGC1404	NGC2976	NGC3621	NGC4594	NGC5457	

### 2.2 PACS Imaging Maps

PACS maps for a total of 60 galaxies are delivered in DR2. The missing galaxy is NGC584, whose observations failed during the first attempt, the re-observations have been obtained a few months ago.

For each galaxy, 3 data cubes, one for each of the PACS bands, are delivered as FITS files. Each data cube contains four or five planes, with the plane index providing the third dimension: the signal map, the uncertainty map, the drifts subtracted during processing, the weight map, and (when present) the signal map built with each scan weighted by its inverse variance (see section 3.3). The Level 2 PACS maps were obtained through

Table 2: Galaxies in the KINGFISH PACS Spectral sample (listed in order of increasing RA)

Name	Strip	Enucs	[NII] 205	Name	Strip	Enucs	[NII] 205
NGC0337	N	0	Y	NGC3521	Y	3	Y
NGC0628	Y	4	Y	NGC3621	Y	0	N
NGC0855	N	0	N	NGC3627	Y	3	Y
NGC0925	Y	0	N	NGC3773	N	0	N
NGC1097	Y	2	Y	NGC3938	Y	2	N
NGC1266	N	0	Y	NGC4254	Y	2	Y
NGC1291	N	0	N	NGC4321	Y	2	Y
NGC1316	N	0	N	NGC4536	Y	0	N
NGC1377	N	0	Y	NGC4559	Y	0	N
NGC1404	N	0	N	NGC4569	Y	0	Y
IC 0342	N	0	Y	NGC4579	Y	0	N
NGC1482	N	0	Y	NGC4594	Y	0	N
NGC1512	Y	0	N	NGC4625	N	0	N
NGC2146	N	0	Y	NGC4631	Y	0	Y
HolmbergII	N	0	N	NGC4725	N	0	N
NGC2798	N	0	Y	NGC4736	Y	1	Y
NGC2841	Y	0	N	NGC4826	Y	0	Y
NGC2915	N	0	N	NGC5055	Y	1	Y
NGC2976	Y	2	Y	NGC5398	N	0	N
NGC3049	N	0	Y	NGC5408	N	0	N
NGC3077	N	0	Y	NGC5457	Y	7	Y
NGC3190	Y	0	N	NGC5474	N	0	N
NGC3184	Y	0	N	NGC5713	N	2	Y
NGC3198	Y	0	N	NGC5866	Y	0	Y
IC 2574	N	0	N	NGC6946	Y	7	Y
NGC3265	N	0	N	NGC7331	Y	0	Y
NGC3351	Y	0	Y	NGC7793	Y	3	N

processing with Scanamorphos (Roussel, 2013, PASP, 125, 1126) of the Level 1 products. The pixel scale of the PACS maps is wavelength-dependent: 1.4 at 70  $\mu\text{m}$ , 1.7 at 100  $\mu\text{m}$ , and 2.85 at 160  $\mu\text{m}$ . The flux units are Jy/pix.

No residual background is removed from the maps. The final maps have orientation North up, East left. See section 3 for more details.

### 2.3 PACS Spectral Maps & Cubes

For each of the 54 galaxies for which PACS line spectroscopy was performed, we deliver spectral cubes and a set of surface brightness maps as FITS files for each targeted emission line. Each image contains an integrated intensity map and an error map, in units of  $\text{W m}^{-2} \text{sr}^{-1}$  as individual extensions. Spectral cubes are also presented as multi-extension FITS files containing a total of 4 extensions: intensity cubes, error cubes, coverage cubes, and a FITS binary table containing the wavelength index associated with each plane of the spectral cube. As we project our data using the a drizzle algorithm, coverage is obtained following Eq. 2 of Fruchter & Hook (2002, PASP, 114, 144). Coverage values are not the amount of time spent on sky per pixel, but rather the sum of the fractional drop areas contributing to the sky pixel brightness.

The final cubes and maps have a pixel scale of  $\sim 2.06, 2.13, 2.31, 2.64,$  and  $3.29$  arc-sec/pixel for [O I], [O III], [N II] 122 $\mu\text{m}$ , [C II], and [N II] 205 $\mu\text{m}$ , respectively, and typical dimensions of  $\sim 55'' \times 55''$  for a map of a single *Herschel* pointing. As the exact pixel scale is determined by the drizzle algorithm, the pixel scale of each cube/map will vary slightly due to different spatial overlaps of AORs. As part of the transient correction, (described in section 4.1) we have removed the underlying continuum from each layer of the cube. The uncertainty maps have the same pointing and calibration as the flux maps.

The maps are in the standard astronomical orientation (North up and East left). See section 4 for more details.

### 2.4 SPIRE Maps

For each of the 61 galaxies, two sets of maps, for a total of 18 maps per galaxy, are delivered as single-extension FITS files. The two sets differ in the mapping software used to produce the Level 2 products: one set is obtained with the HIPE processing pipeline and the other, which we recommend for use, with Scanamorphos (Roussel, 2013).

Within each set, there are three maps for each of the SPIRE bands: one each signal, uncertainty, and coverage maps. The pixel scale of the SPIRE maps is wavelength-dependent: 6 at 250  $\mu\text{m}$ , 10 at 350  $\mu\text{m}$ , and 14 at 500  $\mu\text{m}$ . The flux units are MJy/sr, which were converted from Jy/beam (the output of the HIPE pipeline, see section 5.4). The HIPE maps have a median background removed, and all maps have orientation North up, East left. The uncertainty maps have the same pointing and calibration as the flux maps; the coverage maps have the same pointing as the flux maps. See section 5 for more details.

## 2.5 File Name Convention

For each galaxy, multiple datasets are delivered, with the following formats:

*PACS imaging:* 3 FITS data cubes, one for each PACS band, with name `<name>_scanamorphos_v16.9_pacs< wavelength in  $\mu\text{m}$ >.0.fits`. The content of each plane within the cube is described both in section 2.2 and section 3.3. The preferred name is the NGC, IC, Holmberg (designated 'Ho') or DDO designation followed by the catalog number (with the exception of dwarf B in the M81 group, designated 'M81dwB', see Table 1). The wavelength is 70, 100, or 160  $\mu\text{m}$ .

*PACS Spectroscopy:* 1 multi-extension FITS data cube and 1 multi-extension FITS map, for each spectral line observed, with names `<name>_<line >.fits` and `<name>_<line >.m0.fits`, respectively. The preferred name is the same as described for the PACS imaging, and the line is CII, OIII, OI, NII122, or NII205.

We note that due to the large size of the data set, the cube and map associated with the [O I] observations of NGC 5457 are split into two files which feature the strip and extranuclear regions separately.

*SPIRE imaging:* 18 FITS files, 9 each for the two map processing methods (HIPE or Scanamorphos), and, for each processing method, three files for each SPIRE band, with name: `<name>_kingfish_spire<wavelength in  $\mu\text{m}$ >_v3-0_[hipe/scan][.unc, for uncertainty maps; .cov, for coverage maps].fits`. The preferred name is the same as described for the PACS imaging, and the wavelength is 250, 350, or 500  $\mu\text{m}$ .

## 3 PACS Imaging Data Products & Post-Level-1 Processing

### 3.1 Processing Summary

All targets were observed with the PACS bolometer arrays using the nominal large-scan mode, except IC342 that was observed in parallel mode. The raw data were processed with HIPE v.6 to v.8, mostly following the standard procedure and using the second-level de-glitching method, up to Level 1 products. The non-uniform HIPE version has minor to negligible impact on the final products.

The level-1 data were then reformatted and processed with *Scanamorphos* v. 16.9 (closely preceding the public version 17). The steps performed for this release include the subtraction of the brightness drifts caused by the low-frequency noise (comprising both the thermal drifts of the telescope and detectors and the flicker noise of the bolometers), de-glitching, and the masking of unstable bolometers and brightness discontinuities. The data are weighted by the inverse square high-frequency noise of each bolometer in each scan, and mapped using the gnomonic projection.

More details on the observations can be found in the KINGFISH reference paper by Kennicutt et al. and a full description of *Scanamorphos* is available in Roussel (2013) and

at <http://www2.iap.fr/users/rousseau/herschel>.

### 3.2 Known Features

Some maps show a very faint striped pattern in a portion of the field of view (see Figure 1). This is due to electrical interferences affecting the readout, that cannot be corrected at the moment. Their impact on the map quality is very minor.

The sky background around the galaxies shows faint structures that may not all be real, and are likely caused by drift residuals. Simulations have shown that these artifacts have brightness well below the  $3\sigma$  significance level computed from the error map.

Map edges covered in only one scan direction may be affected by strong drifts that cannot be corrected because there is not enough redundancy. Therefore, the user is advised to quantitatively use only the part of the map with nominal coverage.

### 3.3 Format of the Data Products

For each galaxy and each filter, four or five different planes are assembled into a data cube, the plane index corresponding to the third dimension (Keyword: NAXIS3). The first plane is the signal map, the second plane is the error map (unbiased weighted estimate of the error on the mean brightness), the third plane contains the drifts subtracted during the processing, and the fourth plane is the weight map. When a fifth plane is present, it contains the signal map built with each scan weighted by its inverse variance. It is provided to allow easy identification of residual artifacts (by comparison with the first plane), but in principle it should not be used for photometry.

Each cube is stored into a file conforming to the FITS standard (Wells et al. 1981, A&AS, 44, 363; Hanisch et al. 2001, A&A 376, 359), and can be separated into simple FITS files using an IDL routine (available upon request).

### 3.4 Flux Calibration

The pipeline was run with the V5 version of the PACS flux calibration set, but the maps have been rescaled by the appropriate correction factors to obtain the V6 flux calibration (as indicated in the fits headers by the FLUXCAL keyword).

### 3.5 Map Parameters

The maps are in the standard astronomical orientation (North up and East left). The adopted pixel scale is approximately one fourth of the point spread function full width at half maximum (FWHM), i.e.,  $1.4''$ ,  $1.7''$ , and  $2.85''$  at 70, 100, and 160  $\mu\text{m}$ , respectively. The surface brightness unit is that of the processing output, Jy/pixel. The (small) sky background level has not been removed from the maps, and no adjustment to the pointing was made.

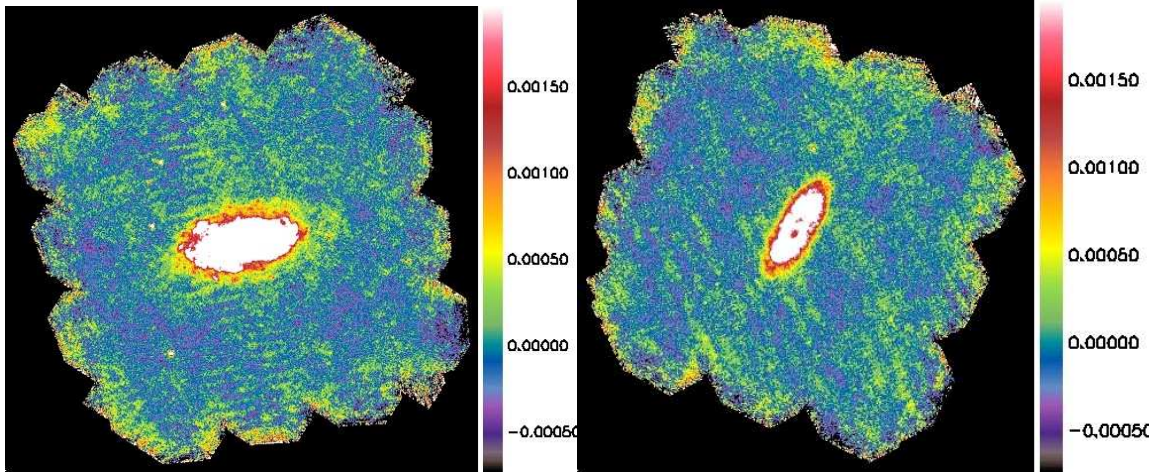


Figure 1: **Known features:** Two examples of electrical interference visible in the maps. The displayed brightness range emphasizes very faint structures (Jy/pixel). For NGC 5055 (left), the pattern is almost parallel to the galaxy major axis. For NGC 2841 (right), it makes an angle of roughly  $45^\circ$  with the major axis.

## 4 PACS Spectral Data Products & Post-Level-1 Processing

### 4.1 Processing Summary

As these are extended objects, all targets were observed with the PACS spectrometer in mapping mode, using the un-chopped grating-scan option. Strips aligned with *Spitzer* IRS long-low observations (Kennicutt et al. 2003; Smith et al. 2007) were observed with a  $n \times 2$  raster pattern using a  $23.5'' \times 4.5''$  step. Extra-nuclear regions, and nuclei for galaxies where a strip was not targeted, were observed with  $2 \times 2$  rastering using a  $4.5''$  step along each axis.

The raw data were processed with HIPE v10 and 11, mostly following standard procedure up to Level 1 products. The non-uniform HIPE version has minor to negligible impact on the final products as all observations were processed with calibration tree version 41. Creation of Level 2 products used a modified version of the standard pipeline. Temporal transients were removed using our own method. We fit the continuum on either side of the expected line and rectified glitches and transients. Initial locations of the emission lines were estimated from HI velocity maps. These locations were iteratively updated using velocity measurements as CII line positions and widths were measured in both PACS and SPIRE/FTS. We then iterated the transient removal with the improved knowledge about the line position. Individual AORs for each galaxy were combined using the same wavelength grid and subsequently projected using the drizzle routine available in HIPE. Error



cubes were constructed based on the RMS spread of data at each location within each wavelength bin. Additional details on the observations can be found in the KINGFISH reference paper by Kennicutt et al. (2011)

The algorithm employed for making integrated emission “moment zero” maps out of the data cubes emphasizes robustness to spectral artifacts. A linear baseline is first removed from the cubes, avoiding the central spectral regions where signal is expected. The wavelength coordinates of the spectral pixels are translated to velocities using the radio definition ( $v/c = (\lambda - \lambda_0)/\lambda = (\nu_0 - \nu)/\nu_0$ ), and an acceptable spectral region for signal to be present is defined for each galaxy based on the known VLSR of the galaxy and its HI linewidth. The signal corresponding to each spatial pixel is then fitted by a single Gaussian (this is a good representation of the instrumental line profile according to the PACS documentation). The results of this fit are accepted or rejected based on a number of criteria designed to avoid fitting spectral artifacts (for example, fits that are judged to yield too broad or too narrow Gaussians are rejected, as are fits that show significant excess uncertainty over the expected noise, indicating a non-Gaussian profile). Following this step, the pixels with failed Gaussian fits are filled in the maps with simple velocity integrations over a narrow range of channels. The central velocity for these integrations is chosen based on the fitting results for the nearest neighbors with a valid fit for the [CII], or using the [CII] central velocity and velocity width results as a guide for the rest of the transitions (which are usually considerably fainter and less widespread). The uncertainty of the signal is evaluated using the RMS of the spectrum in the regions devoid of signal as an estimator of the error in one velocity channel. This error is propagated accordingly through the fit or the velocity integration used.

## 4.2 Known Features

The edges of line maps may exhibit some blockiness. This is a result of diminished coverage away from the center of the raster pattern. Some maps featuring extended strips may exhibit a striped pattern along the strip. This is seen more frequently in [O I] and [O III] maps with low S/N. These striped regions result in pixels with a higher level of noise which appears to be associated with one of the spatial-pixels in the blue detector.

## 4.3 Format of the Data Products

The output of our pipeline is 2 files for each line observed in each galaxy. One file contains the maps associated with the zeroth moment map while the other contains the data cubes from which the moment map was constructed.

## 4.4 Map Parameters

The maps are in the standard astronomical orientation (North up and East left). The adopted pixel scale is approximately one fourth of the point spread function full width at



half maximum (FWHM), i.e.,  $1.4''$ ,  $1.7''$ , and  $2.85''$  at 70, 100, and 160  $\mu\text{m}$ , respectively. While cubes have a surface brightness unit derived from the processing output,  $\text{Jy}/\text{pixel}$ , maps have been converted into  $\text{W m}^{-2} \text{sr}^{-1}$ . No adjustment to the pointing was made.

## 4.5 Comparison with ISO

Where possible, comparisons were made between the line fluxes obtained with KINGFISH and those obtained with the Long Wavelength Spectrometer aboard the Infrared Space Observatory. Secure [C II] 158  $\mu\text{m}$  and [O I] 63  $\mu\text{m}$  data were obtained for a total of 24 KINGFISH galaxies with both Herschel and ISO. For this subset of the KINGFISH sample a detailed comparison in the lines fluxes was made.

An important difference between the Herschel and ISO data is the discrepant beam size between the two observatories. For example, the ISO-LWS PSF has FWHMs of  $\sim 87''$  at 63  $\mu\text{m}$  and  $\sim 70''$  at 158  $\mu\text{m}$ , much larger than the  $6''$  and  $11''$  Herschel beams at these wavelengths. Another major complication is the large uncertainty in the so-called ISO-LWS aperture correction, which is a factor of  $\sim 2$  for extended sources (see Brauher et al. 2008 for details). A third issue in executing such a cross-observatory comparison is the difference in the spatial coverages between the ISO-LWS and Herschel PACS data.

The first step in carrying out the comparative analysis was to account for the difference in spatial coverage in the Herschel and ISO line data. This was achieved by inserting our PACS spectral line maps into our PACS images (the 70  $\mu\text{m}$  image for the [OI] 63  $\mu\text{m}$  map and the 160  $\mu\text{m}$  image for the [CII] 158  $\mu\text{m}$  map), after first scaling the PACS images to match the amplitudes of the PACS line maps. Then LWS-esque line fluxes were extracted from the enlarged line maps via

$$\text{line flux} = \pi\theta^2[\text{Sum}_i f_i w_i]/[\text{Sum}_i w_i], \quad (1)$$

where  $\theta$  is the ISO-LWS beam size,  $f_i$  is the surface brightness of pixel  $i$ , and  $w_i$  is the amplitude of the ISO-LWS PSF at pixel  $i$ 's radial distance from the center of the ISO-LWS pointing. In comparing these Herschel-based line fluxes to those from Brauher et al. (2008), we find a scatter of a factor of  $\sim 2$  in their ratio. In light of the large uncertainties in the comparison (including a factor of  $\sim 2$  in the extended source aperture correction), the results from the two observatories are consistent.

## 5 SPIRE Imaging Data Products & Post-Level-1 Processing

### 5.1 Introduction

The KINGFISH SPIRE maps are created from multiple Herschel scans obtained in the SPIRE photometric mode (with the exception of IC342, which was measured in the SPIRE/PACS parallel mode), and fully processed with HIPE v.8 up to Level 1 products. For the Level 2 products, both HIPE v.8 and *Scanamorphos* v. 16.9 are used, and maps obtained with

both types of processing software are delivered in DR2. Portions of the HIPE pipeline have been modified to mask out the galaxy when measuring the background, to increase the size of the map by adding the data taken while the spacecraft turns around after each scan leg, and to adjust the pointing. The KINGFISH observing strategy is to map each galaxy with two scanning directions oriented at approximately right angles to each other, with 2 (for targets with  $S_{160}$  at  $R_{25} > 3$  MJy/sr) or 4 (for targets with  $S_{160}$  at  $R_{25} \leq 1$  MJy/sr) repetitions (same pattern) for each, out to 1.5 times the optical radius.

## 5.2 Calibration Addendum: Changes Between DR2 and DR3

Over the year since DR2, the SPIRE Instrument Team has revised its estimate for the effective beam size for each of the 3 SPIRE bands. For extended sources, such as the KINGFISH galaxies, the net effect is to *lower* intensities in SPIRE250, SPIRE350, and SPIRE500 by factors of 0.9282, 0.9351, and 0.9195, corresponding to fractional changes of -6.2%, -6.5%, and -8.1%.

A quick fix for the user of the KINGFISH DR2 SPIRE maps is to multiply the maps by factors 0.9282 (SPIRE250), 0.9351 (SPIRE350), and 0.9195 (SPIRE500).

For more information, please refer to the document posted at:  
[http://www.astro.princeton.edu/~draine/Notes\\_re\\_KINGFISH\\_SPIRE\\_Photometry.pdf](http://www.astro.princeton.edu/~draine/Notes_re_KINGFISH_SPIRE_Photometry.pdf)

## 5.3 Data Products

The output of our pipeline is 18 FITS files for each galaxy: 3 products (the calibrated image, the uncertainty, and the coverage map) for each of the 3 bands, processed twice: with HIPE and *Scanamorphos*.

## 5.4 Image Processing

The raw KINGFISH SPIRE data are processed through the early stages of HIPE to calibrate the data in physical units. For the data that will be processed further in HIPE, a line is fit to the data for each scan leg after masking out the galaxy, and this fit is subtracted from the data. Discrepant data (usually a rogue bolometer, of which there are  $< 1$  per map, on average) are also masked, and the data (plus the turnaround region, for the  $\sim 90\%$  of the sample that didn't have visible streaks in that region) are mosaicked using the native mapper in HIPE. These steps are not required for the data processed with *Scanamorphos*, which automatically performs the matching or rejecting of data. The map coordinates of both *Scanamorphos* and HIPE products are then adjusted so that the average position of the point sources (measured using StarFinder; Diolaiti et al. 2000, SPIE, 4007, 879) match those in the MIPS 24  $\mu\text{m}$  images. This adjustment averaged  $3''$  and had a Gaussian distribution characterized by a standard deviation of  $3''$ , which we take to be the pointing uncertainty. Finally, the images are converted to surface brightness units (MJy/sr), con-

verted from Jy/beam (the output of both the HIPE pipeline and *Scanamorphos*) using the beam areas recorded in the image headers.

**Photometric Uncertainties** Currently the estimated calibration uncertainties, from the SPIRE Observer's Manual 2010, are 7%. The uncertainty in the beam size is  $\sim 1\%$ , and when added in quadrature with the calibration uncertainty results in a total uncertainty still of  $\sim 7\%$ .

## 5.5 Comparison with DR1 SPIRE Maps

The DR2 SPIRE maps look very similar to those of DR1, with the new products slightly ( $\sim 2\%$  at 250 and 350  $\mu\text{m}$ ) to moderately ( $\sim 10\%$  at 500  $\mu\text{m}$ ) fainter than those in the previous delivery. The backgrounds of the maps processed with *Scanamorphos* can be quite different from those of the maps processed with HIPE, since *Scanamorphos* does not force a background removal, which is instead implemented on the HIPE maps. The beam reconstructed by *Scanamorphos* is slightly (3%) larger than in DR1, as reflected in the 'BEAMSIZE' parameter in the image headers.